REDUCED GAIN PI/PID CONTROLLERS
FOR FOPTD/SOPTD PROCESSES UNDER LOAD DISTURBANCE

Andrzej BOŻEK*, Leszek TRYBUS*

*Faculty of Electrical and Computer Engineering, Department of Computer and Control Engineering,
Rzeszow University of Technology, al. Powstańców Warszawy 12, 35-959 Rzeszów, Poland

abozek@prz.edu.pl, ltrybus@prz.edu.pl

Abstract: In practical applications, an engineer is sometimes expected to execute the step test for tuning the controller without waiting much for the steady-state or a low level of disturbances. Hence, knowing that the initial settings may not be quite reliable, he/she detunes the controller by reducing its gain as a precaution against possible poor behaviour of the closed-loop system. It is up to their experience to choose by how much to detune. Therefore, the development of a practically oriented approach that would assist the engineer to choose the degree of gain reduction is the goal of this paper. The approach assumes that process parameters are determined by the least-squares approximation of the step response. Accuracy of the approximation is evaluated by a relative approximation error involving integrals of the error and the process response itself. The SIMC tuning rules are applied to choose the initial controller settings. The approach relies on detecting by simulation the worst case that may happen when the step response is triggered at any time. Detuning nomograms specify by how much to reduce the initial gain for PI-FOPTD and PID-SOPTD designs, given the relative approximation error. Two long-lasting lab experiments involving temperature control identify a plant, verify the load disturbance model through multiple step tests and demonstrate usage of the approach in the closed-loop system.

Key words: load disturbance, process identification, controller tuning, SIMC, FOPTD, SOPTD

1. INTRODUCTION

Two types of disturbances are distinguished in industrial processes controlled by automation systems. The first one affects the state of the process, similar to the control input, whereas the other one only corrupts the output. Examples of the first type include disturbances of the load, fluctuations of raw material composition, power supply and ambient temperature usually jointly called a load disturbance [1,2]. Measurement noise dependent on transducer data, electromagnetic interference, and grounding quality is the other type. The load disturbance affects the process at low frequencies (LF), whereas the measurement noise interferes at high ones.

To suppress the effect of the disturbances, a process controller, typically PI or PID, must be reasonably well tuned, which in industrial practice is done experimentally by means of the step response or relay feedback [3]. In the case of the former, the parameters of the process are identified from the response and used to calculate controller settings. A steady-state and low level of disturbance, particularly the load disturbance, are the conditions required to obtain a trustworthy response and reliable parameters. The use of parameters acquired from a response triggered not at suitable conditions may lead to unreliable settings and poor behaviour of the closed-loop system.

However, in industrial applications, it is difficult to know whether the process to be identified is in a steady-state or not disturbed. In addition, waiting for such a steady-state can be cumbersome for a process with a long time constant or delay [4]. Therefore, an engineer has to sometimes execute the test when-ever technology permits, without much waiting. Nevertheless, as a precaution, he/she does not apply the initial settings directly but detunes the controller by reducing its gain. The degree by how much to detune is determined by the rule of thumb.

Therefore, the purpose of this paper is to develop a practically oriented approach that will determine to what extent to reduce the gain in controller settings obtained from the response triggered at any time of process operation. A relative difference between the response and its least-squares approximation is the basic data for reducing the gain. SIMC tuning rules are applied to calculate the settings [2,5].

To justify the solutions used in the approach, we begin with a review of related work on process identification and SIMC tuning.

1.1. Process identification for load disturbance

A tutorial review of identification methods dealing with measurement noise and load disturbance is presented in Ref. [4]. In the presence of a general form of measurement noise, such as coloured noise, the least-squares solutions do not give unbiased parameter estimates [6]. To solve the bias problem, the instrumental variable (IV) method that adjusts the estimates in a few stages can be applied [7]. As far as the load disturbance is concerned, the problem of using the step response data while the output is not initially in a steady-state may be overcome by including the initial state and its derivatives into the identified parameters, yet assuming no load disturbance [8]. If, besides the initial conditions, the output is corrupted by measurement noise, the IV method can be applied [9].

If the load disturbance description is known a priori, then the output may be decomposed into perturbed and unperturbed components, so as to obtain unbiased parameters of the process while estimating the dynamics of the disturbance response [10]. For example, a period of the perturbed component may be detected in this way [11]. No prior information is required if the perturbed component is treated as a dynamic parameter for estimation. A recursive least-squares algorithm is needed in such a case [12]. The perturbed component can also be estimated by correlation analysis [13].

Finally, no knowledge on the initial conditions or the load disturbance description is required if curve-fitting algorithms with quasi-Newton iterations are applied [6,7]. Both open and closed loops can be handled in this way, as demonstrated in Ref. [14] for an industrial application. In the case of overdamped systems with delay, each curve fitting iteration consists of two stages in which process parameters and the delay are estimated separately [15,16].

An approach is also proposed to calculate the process gain first from a steady-state change and then the time constant along with process delay in the second stage [17]. Good performance is reported for indirect identification of continuous delay systems based on discrete-time models [18]. Efficient identification from a low-quality step response by means of regularised least-squares is recommended in Ref. [19].

1.2. SIMC tuning rules

The selection of PI and PID tuning rules is another relevant issue. Note that to evaluate by how much the controller should be detuned, some quantification of the closed-loop behaviour is needed. Indicators of such behaviour include settling time, overshoot, peak time, IAE [20] or ITAE [21] integral, and relative delay margin [22]. However, among a large number of tuning rules collected in Ref. [23], only a fraction expresses controller settings not only in terms of process parameters, but also by a design specification related to the closed-loop behaviour.

The idea of using a desired closed-loop time constant to design a discrete controller was first introduced in Ref. [24], where this time constant was denoted by λ. Later, the approach was adapted to the internal model control (IMC) and PID controller [25]. In the case of the first- or second-order-plus-time-delay processes, i.e. FOPTD or SOPTD, the so-called SIMC tuning rules [2,5,26] express PI and PID settings in terms of the process parameters and the desired λ. This enables an engineer to choose how aggressive the controller should be. Due to simplicity, the SIMC rules have been widely approved in industrial practice [2]. Naturally, if due to disturbances, the identified parameters are unreliable, the value of λ must be increased to avoid poor closed-loop behaviour.

Performance of the SIMC rules for set-point and load disturbance responses can be assessed using the IAE, leading to some modification of the approach [26]. Minimisation of the IAE also enables to apply other closed-loop indicators for design. This is demonstrated in Ref. [27], where a weighted average of the IAEs for set-point and load disturbance responses is minimised subject to sensitivity constraints. A similar approach is used in Ref. [28] to improve disturbance rejection, but without applying the pole-zero cancellation of the original SIMC.

1.3. Outline of the approach

The development is based on a long uninterrupted MATLAB simulation of FOPTD and SOPTD disturbed processes, where step responses are continuously triggered one after another. Load disturbance is simulated by a low-pass filter driven by white noise. Measurement noise is treated as filtered out noise [29].

By repeating the simulation for different process delays, final nomograms specify the degree of reducing the gain for PI-FOPTD and PID-SOPTD designs in terms of a relative approximation error of the step response. Practical usage of the approach is demonstrated in a dedicated lab set up enabling repeatable tests in a long time period. The set up involves a temperature control plant, similar to the one in Ref. [30], whose dynamics can be well approximated by the FOPTD model. The load disturbance model is also verified from the tests.

The paper is organised as follows. The next section introduces normalised FOPTD and SOPTD process models affected by low-frequency load disturbance. The single, long simulation consists of multiple (5,000) up–down step tests resulting in 10,000 responses approximated by the curve fitting. Accuracy of the approximation is determined by a relative approximation error defined as the ratio of two integrals over time of the response. The first one integrates absolute estimation error and the second one involves the process response itself.

SIMC settings for PI-FOPTD and PID-SOPTD are given in Section 3 by taking the desired closed-loop time constant equal to the process delay [5]. Having the settings, the expected closed-loop behaviour can be inferred by calculation of the gain margin [31].

Controller settings and the corresponding gain margins are evaluated in Section 4 for each of the simulated responses. A minimum margin represents most inconvenient behaviour of the closed-loop system (worst case). This also enables to detect the maximum error for which the SIMC rules do not yet lead to instability. A worst case plant stabilised by means of an IMC-based PID controller is also considered in Ref. [32].

The difference between the nominal gain margin and the minimum margin determined above indicates by how much the design margin should be increased to avoid poor behaviour. In turn, that difference is converted in Section 5 into the corresponding reduction factor of the controller gain, expressed by respective nomograms for PI-FOPTD and PID-SOPTD designs.

The approach is verified in Section 6 by two long lab experiments, one for open loop and the other for closed loop, involving a heating resistor kept in open air. As in the MATLAB simulation, each experiment consists of multiple up–down step responses triggered in the presence of load disturbances. The time constant of the low-pass filter as a disturbance model is evaluated to justify the value used in the earlier sections.

2. PROCESS MODEL AND IDENTIFICATION

2.1. Process and load disturbance

A simulated process given in Fig. 1(a) is considered, where u denotes the control input, y the output and l the load disturbance interfering at LFs. High frequency (HF) measurement noise m is dropped from the simulation, although in the lab experiment, the

filtered m increases the effect of l. The following transfer functions

$$G_{\text{FOPTD}}(s) = \frac{k}{Ts+1}e^{-\tau s}, \quad G_{\text{SOPTD}}(s) = \frac{k}{(Ts+1)^2}e^{-\tau s} \quad (1)$$

represent the FOPTD and SOPTD process models (with different values of the parameters $k, T,$ and τ). Due to the double time constant in SOPTD, the two models are consistent in terms of the parameter set $\{k, T, \tau\}$. Different time constants for SOPTD are not considered as they would require much longer control input to get identified values reasonably close to true ones.

Settling times can be expressed as $4T + \tau$ and $6T + \tau$, respectively, or $5T$ and $7T$ for $\tau \leq T$. In practice, due to the disturbance, the step response is recorded for somewhat a longer time to be sure about the settling. Therefore, here, we take the double step-response settling time, i.e. $10T$ for FOPTD and $14T$ for SOPTD, as the identification time horizon.
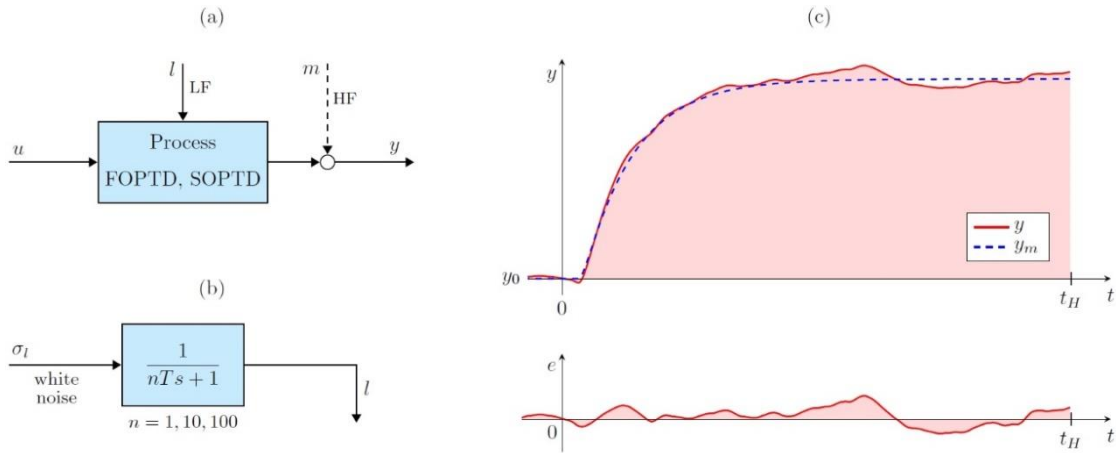

Fig. 1. (a) Process model, (b) load disturbance model, (c) step responses of the process y and model y_m, estimation error e
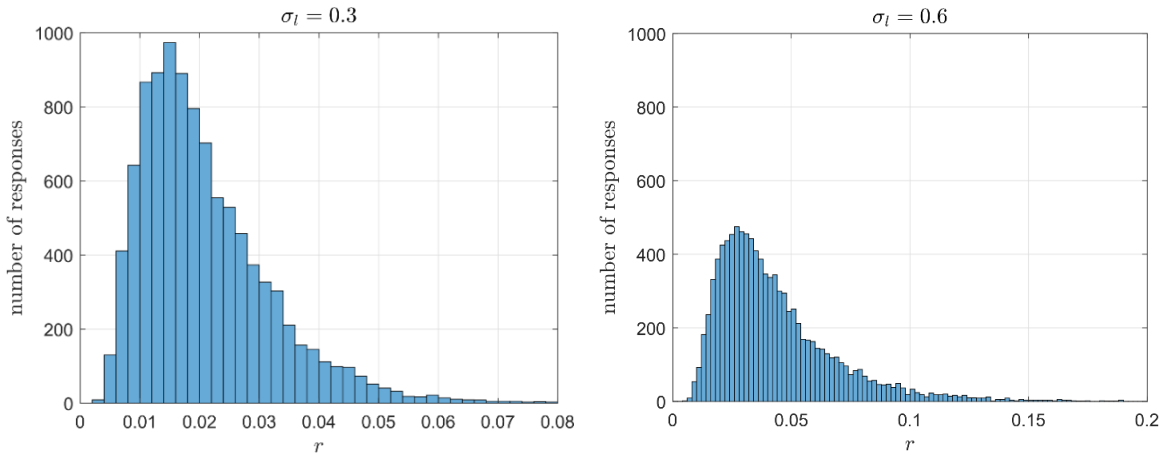

Fig. 2. Number of step responses in terms of the relative approximation error r
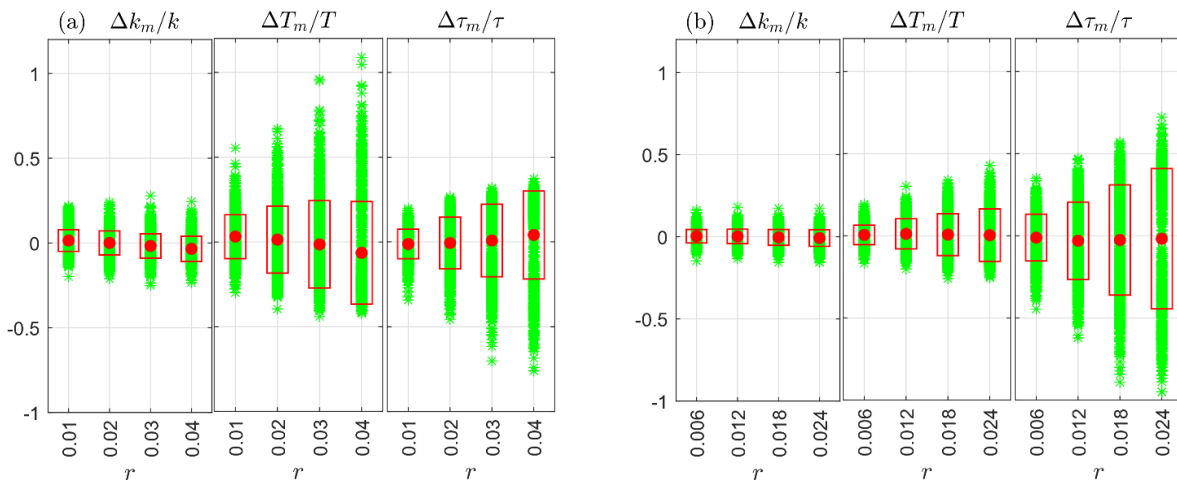

Fig. 3. Relative deviations of the parameter estimates for (a) FOPTD, $\sigma_l = 0.3$, (b) SOPTD, $\sigma_l = 0.15$

The LF load disturbance l is generated by the low-pass filter shown in Fig. 1(b), with the time constant n-times longer than the process. The results presented in the following sections refer to $n = 10$. Although it would be more appropriate to call the $n = 1$ case a "medium frequency" and not LF, it is left in the study for comparison. The level of l is adjusted by means of the standard deviation σ_l of the white noise driving the filter. A sample step response y of the disturbed process is shown in Fig. 1(c), where t_H denotes the identification time horizon.

2.2. Relative approximation error

The least-squares curve fitting the MATLAB lsqcurvefit function is used for identification, since the autoregressive arx and the instrumental variable iv4 cannot deal with the load disturbance [6,7]. Let $\{k_m, T_m, \tau_m\}$ denote the parameter estimates of the identified model, y_m its step response and $e = y - y_m$ the estimation error. The integrals

$$Y = \int_0^{t_H} |y(t) - y_0| \mathrm{d}t, \ E = \int_0^{t_H} |e(t)| \mathrm{d}t, \tag{2a}$$

representing the shaded areas in Fig. 1(c) determine the ratio

$$r = \frac{E}{Y} \tag{2b}$$

treated as an indicator to what extent the response is deformed by the load disturbance. The ratio, termed here a relative approximation error, is a basic data for detuning.

Realistic values of r for which parameter deviations from true values are not too large are below 0.05 for FOPTD and 0.03 for SOPTD. Larger deviations may cause instability of the closed-loop system tuned according to the SIMC rules [5] or excessive sluggishness in the case of the detuned controller (Section 5). Hence, trustworthy SOPTD responses require a smaller level of the load disturbance. If r of a particular real response turns out too high, it may be reduced in the next response by increasing the input step (if technology permits).

2.3. Simulation methodology and parameter estimates

Consider a continuously operating real process that can be tested any time by a step response. Meanwhile, the process can be perturbed by the load disturbance to a varying degree. An equivalent of such a process is implemented here in the form of a long uninterrupted simulation involving either the FOPTD or the SOPTD model, with the disturbance generated as shown in Fig. 1(b). During this simulation, step responses are triggered one after another, characterised by their own relative approximation error (2b). It turns out that about 10,000 tests are needed in the simulation to get histograms of r with fairly repeatable shape (see Fig. 2).

The results presented in the paper refer to the normalised time-constant-scaled process model, i.e. for $k = 1$, $T = 1$, and τ in the typical interval $[0.1, 1]$ (e.g. Ref. [31]). Some figures refer to $\tau = 0.32$ (middle of the decade). If T_m and τ_m are raw estimates of the parameters, then $\tau = \tau_m / T_m$.

Two histograms of the number of responses in terms of the error r for basic and twice increased standard deviation σ_l of the load disturbance are shown in Fig. 2 for FOPTD. Increase of σ_l extends the range of r while decreasing the maximum.

Roughly comparable deviations of the parameter estimates from true values are shown as bar graphs in Figs. 3(a) and (b) for FOPTD and SOPTD, respectively. Naturally, the deviations grow with the relative error r. Dots in the middle of the bars are means, and rectangle heights denote two standard deviations. The ranges $r = 0.04$ for FOPTD and 0.024 for SOPTD correspond to the load disturbance deviations $\sigma_l = 0.3$ and 0.15. This indicates that a similar degree of confidence in the SOPTD model as in the FOPTD requires a significantly lower disturbance level.

3. GAIN MARGIN FOR SIMC-BASED PI AND PID

Suppose for the time being that no load disturbance affects the process. The popular SIMC tuning rules used here express PI and PID settings in terms of the parameters $\{k, T, \tau\}$ and a desired closed-loop time constant λ [2,5].

Consider first the FOPTD process in Eq. (1) for which the PI controller

$$G_{PI}(s) = k_p \left(1 + \frac{1}{T_I s}\right) \tag{3a}$$

suffices. Given the desired λ, the SIMC rules are as follows

$$k_P = \frac{1}{k} \frac{T}{\lambda + \tau}, \quad T_I = T. \tag{3b}$$

Skogestad in Ref. [5] recommends

$$\lambda = \tau \tag{4}$$

to get a tight response, whereas $\lambda = 1.5\tau$ provides a smoother response and $\lambda = 0.5\tau$ a more aggressive one. Some reduction of T_I for the large time constant T improves the reaction to the load disturbance [5,27]. However, we remain with the recommended Eq. (4) to preserve simplicity.

For Eq. (4), the rules become

$$k_P = \frac{1}{k} \frac{T}{2\tau}, \quad T_I = T \tag{5}$$

and the open-loop transfer function for $G_{FOPTD}(s)$ obtains the simple form

$$G_{open}(s) = G_{PI}(s) G_{FOPTD}(s) = \frac{1}{2\tau s} e^{-\tau s} \tag{6}$$

due to pole-zero cancellation. Since the plant model is not known exactly, the cancellation is not perfect. Therefore, some reduction of the gain k_P is needed to avoid possible oscillations (Section 5).

Gain margin $GM = 1/|G_{open}(j\omega_{GM})|$ is determined by the frequency ω_{GM} obtained from the angle condition $\angle G_{open}(j\omega_{GM}) = -\pi$. In the case of Eq. (6), we have $\angle G_{open}(j\omega_{GM}) = -\pi/2 - \tau\omega_{GM}$, which yields

$$\omega_{GM} = \frac{1}{\tau} \frac{\pi}{2} \text{ and } |G_{open}(j\omega_{GM})| = \frac{1}{\pi}. \tag{7}$$

So, for the PI-FOPTD design, we get

$$GM = \pi. \tag{8a}$$

Gain margin expressed in decibels will also be used, so

$$GM_{dB} = 9.94 \text{ dB} \cong 10 \text{ dB}. \tag{8b}$$

For the SOPTD process in Eq. (1) and the PID controller,

$$G_{PID}(s) = k_p \left(1 + \frac{1}{T_I s} + T_D s\right) \tag{9a}$$

the SIMC rules have the form [2,5]

$$k_P = \frac{1}{k}\frac{2T}{\lambda+\tau}, \quad T_I = 2T, \quad T_D = \frac{T_I}{4}. \tag{9b}$$

Then the controller becomes

$$G_{\text{PID}}(s) = k_P\frac{(Ts+1)^2}{2Ts}, \tag{10a}$$

where for the recommended $\lambda = \tau$, we get

$$k_P = \frac{1}{k}\frac{T}{\tau} \tag{10b}$$

and the transfer function $G_{\text{open}}(s) = G_{\text{PID}}(s)G_{\text{SOPTD}}(s)$ retains the form Eq. (6), so the margin GM or GM_{dB} is the same as before.

4. GAIN MARGINS FOR THE IDENTIFIED MODELS

4.1. Gain margin and relative approximation error

Let $\{k_m, T_m, \tau\}$ denote parameter estimates obtained from one of the disturbed responses characterised by a relative approximation error r in Eq. (2b). In the case of the PI-FOPTD design, we have

$$k_P = \frac{1}{k_m}\frac{T_m}{2\tau_m}, \quad T_I = T_m \tag{11}$$

from Eq. (5). Since the simulated process is given in the normalised form $e^{-\tau s}/(s+1)$ (Section 2), the open-loop transfer function becomes

$$G_{\text{open}}(s) = k_P\frac{T_I s+1}{T_I s}\frac{1}{s+1}e^{-\tau s}. \tag{12}$$

The angle condition $\angle G_{\text{open}}(j\omega_{GM}) = -\pi$ results in the equation

$$\frac{\pi}{2} + \text{arctg}(T_I\omega_{\text{GM}}) - \text{arctg}\,\omega_{\text{GM}} - \tau_m\omega_{\text{GM}} = 0 \tag{13a}$$

for the frequency ω_{GM}. After solving Eq. (13a), the corresponding gain margin is calculated as

$$\text{GM} = \frac{T_I\omega_{\text{GM}}}{k_P}\sqrt{\frac{\omega_{\text{GM}}^2+1}{(T_I\omega_{\text{GM}})^2+1}}. \tag{13b}$$

The bar graph in Fig. 4 presents the margin GM_{dB} in terms of the relative error r. Each bar consists of 1,000 points. Although the means are close to 10 dB, there are cases with quite small or even negative margins. The approximating parabolic curve $\text{GM}_{\text{dB,m}}(r, \tau = 0.32)$ specifies the minimum value of the margin in terms of the relative error. The minimum is defined here as three standard deviations below the mean. So, a few outliers in Fig. 4 are left out. From the controller's viewpoint, $\text{GM}_{\text{dB,m}}$ indicates the worst case among the step responses having the same relative error r. The value of $\text{GM}_{\text{dB,m}}$ is used in the next section to determine the degree of detuning.

Note that besides the main curve (continuous line) in Fig. 4 obtained for $n = 10$ in the low-pass filter of Fig. 1(b), there are also two other curves corresponding to the filters with $n = 1$ and 100. These two curves are fairly close to the main one. This confirms that the low-pass filter with $n = 10$ can be an appropriate model of the load disturbance interfering at LFs.
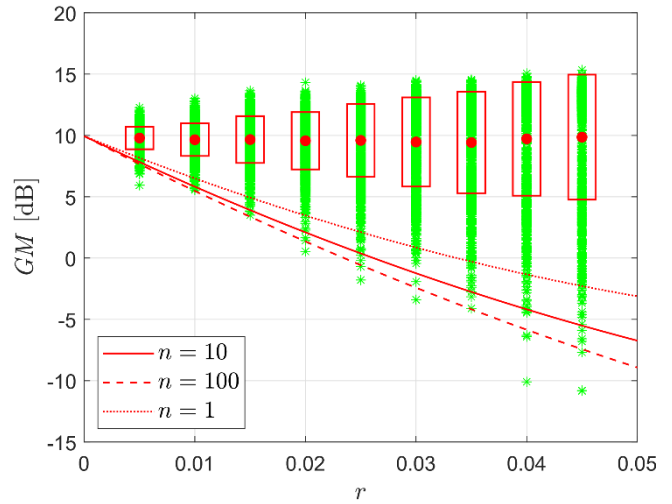

Fig. 4. PI-FOPTD gain margin as a function of the relative approximation error r for $\tau = 0.32$

4.2. Stability limit

By repeating the simulation and calculations for other delays $\tau \in [0.1, 1]$, a few functions $\text{GM}_{\text{dB,m}}(r, \tau)$ of the minimum gain margin shown in Fig. 5 are obtained. Increase of τ reduces the slope of the plots. Note that for $\tau < 0.56$, there exists a certain $r_{\max}$ for which $\text{GM}_{\text{dB,m}}$ becomes zero, which means stability limit. Hence for

$$r > r_{\max,} \tag{14}$$

detuning the controller becomes a necessity. The stability limit function $r_{\max}(\tau)$ is shown in Fig. 6. As seen, $r_{\max}$ increases with τ, which indicates more favourable conditions for identification.

Similar plots $\text{GM}_{\text{dB,m}}(r, \tau)$ and the function $r_{\max}(\tau)$ can be obtained for the PID-SOPTD design. About two times smaller values of $r_{\max}$ for PID-SOPTD in Fig. 6 translate into more demanding conditions for the step tests, i.e. lower level of the load disturbance.
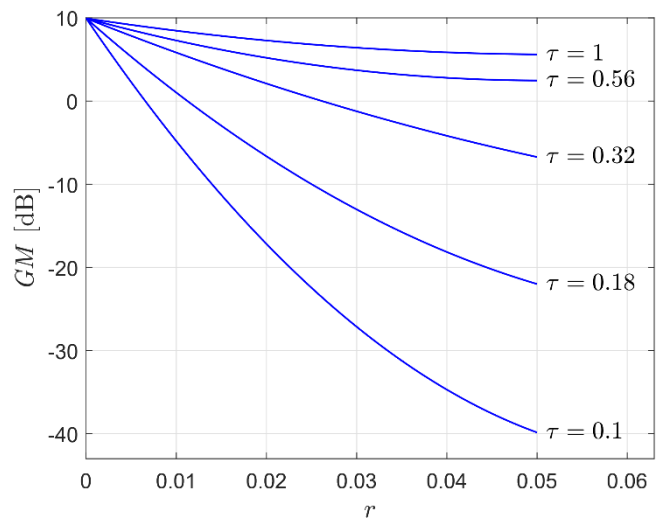

Fig. 5. PI-FOPTD minimum gain margin. $\text{GM}_{\text{dB,m}}$ as a function of r

sciendo

DOI 10.2478/ama-2024-0025

acta mechanica et automatica, vol.18 no.2 (2024)
Special Issue "Modern Trends in Automation and Robotics in tribute to Professor Tadeusz Kaczorek"
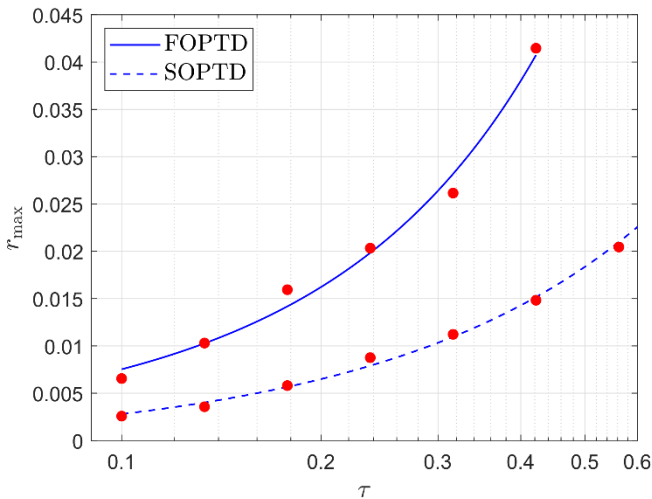
Fig. 6. Relative approximation error $r_{\max}$ for stability limit

5. REDUCTION OF THE CONTROLLER GAIN

While gain margins above $\mathrm{GM_{dB,m}} \cong 10$ dB (Fig. 4) can be accepted since they indicate aperiodic responses, the ones below 10 dB rather not due to possible overshoots, oscillatory transients or even instability. The plots $\mathrm{GM_{dB,m}}$ developed earlier determine the minimum margin that may occur for a particular relative approximation error r.

To avoid poor behaviour due to the insufficient gain margin, the design margin should be moved up by the difference between

the desired nominal value $\mathrm{GM_{dB}}$ and the worst case minimum value $\mathrm{GM_{dB,m}}$. This can be done by replacing k_P in Eq. (11) by κk_P, where $\kappa \le 1$ is the detuning factor.

Before the reduction, we have

$$G_{\mathrm{open}}(s) = k_P G'_{\mathrm{open}}(s) \tag{15}$$

with

$$\mathrm{GM_{dB,m}} = 20 \log_{10} \frac{1}{k_P |G'_{\mathrm{open}}(j\omega_{\mathrm{GM}})|}. \tag{16}$$

The reduction is supposed to restore the nominal gain margin $\mathrm{GM_{dB}}$, so

$$\mathrm{GM_{dB}} = 20 \log_{10} \frac{1}{\kappa k_P |G'_{\mathrm{open}}(j\omega_{\mathrm{GM}})|}. \tag{17}$$

Subtracting Eq. (17) from Eq. (16) gives

$$\mathrm{GM_{dB,m}} - \mathrm{GM_{dB}} = 20 \log_{10} \kappa, \tag{18}$$

hence

$$\kappa = 10^{(\mathrm{GM_{dB,m}} - \mathrm{GM_{dB}})/20}. \tag{19}$$

The nomogram of the gain reduction factor κ in terms of the relative approximation error r and process delay τ is shown in Fig. 7(a) for PI-FOPTD. The value of κ decreases with r and increases with τ. Dots indicate $r_{\max}$, i.e. the stability limit from Fig. 6, where κ equals $1/\pi \cong 0.32$ according to Eq. (8a). Thus, having r and τ for a particular step response, one can read out κ from the nomogram and reduce the initial controller gain.
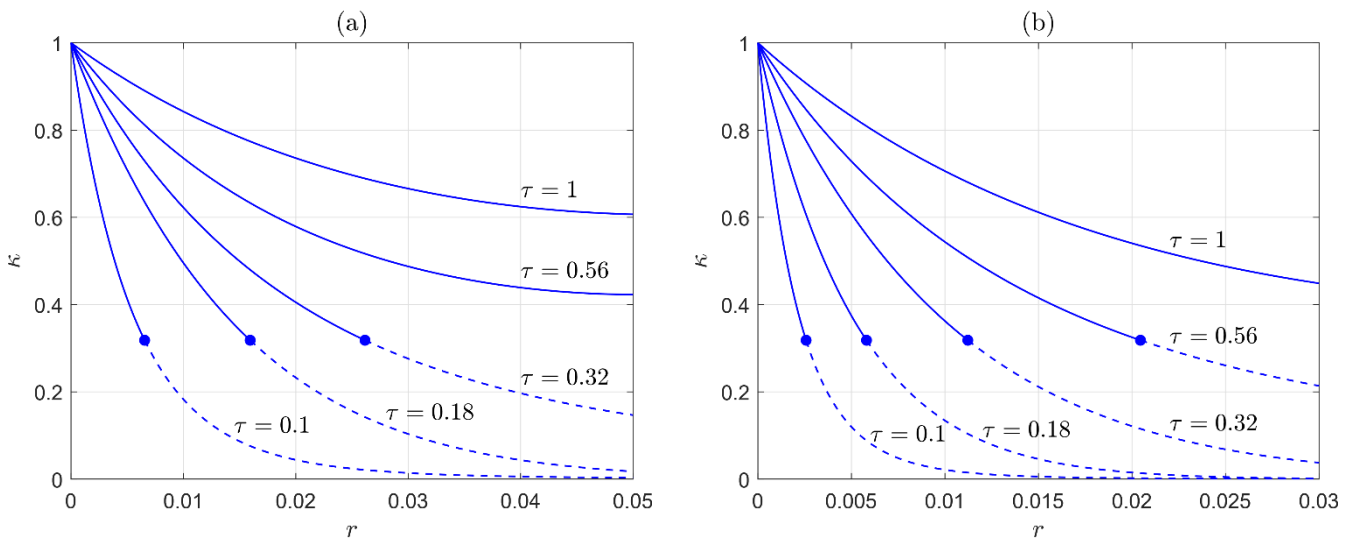

Fig. 7. Gain reduction factor κ of SIMC-based design for: (a) PI-FOPTD, (b) PID-SOPTD

The analogous nomogram for PID-SOPTD is given in Fig. 7(b) with a smaller range of the relative error r. At the first glance, for small r, both PI and PID could be applied. However, a more careful comparison of the nomograms reveals that the reduction factor κ for PID-SOPTD is much smaller than for PI-FOPTD. For instance, if $\tau = 0.32$, the error $r = 0.01$ yields $\kappa = 0.36$ for PID-SOPTD and 0.62 for PI-FOPTD. Only for very small r, the difference becomes negligible. This is another explanation why PI is most often preferred over PID in process control.

The nomograms determine the reduction factor κ also beyond the stability limit, i.e. for $r > r_{\max}$. However, since the proposed approach is worst-case-based, some of the closed-loop responses may turn out excessively sluggish for large r. In particular, it refers to the cases where the gain margins $\mathrm{GM_{dB}}$ are above the nominal 10 dB (see Fig. 4), which indicates slow responses. Reduction of the gain makes them even slower. Unfortunately, for any disturbed step test, the gain margin is not known as to whether it is above or below 10 dB. Therefore, to avoid too slug-

gish responses, we recommend to accept only such step tests that satisfy the condition

$$r < r_{\max}, \qquad (20)$$

with $r_{\max}$ given in Fig. 6. This excludes the tests with too large an approximation error.

The proposed approach is summarised in the form of a natural algorithm in Fig. 8. From the recorded step response, the model parameters, the time-scaled delay τ and the relative approximation error r are first obtained. The parameter $r_{\max}$ is then determined from the nomogram in Fig. 6. If the condition $r < r_{\max}$ is met, controller settings are given by the SIMC rules, followed by the gain reduction according to one of the nomograms in Fig. 7. Otherwise, if possible, the step response is repeated for an increased control step. If not, an engineer must wait for more favourable process conditions. The smooth closed-loop response is expected after completing the procedure.
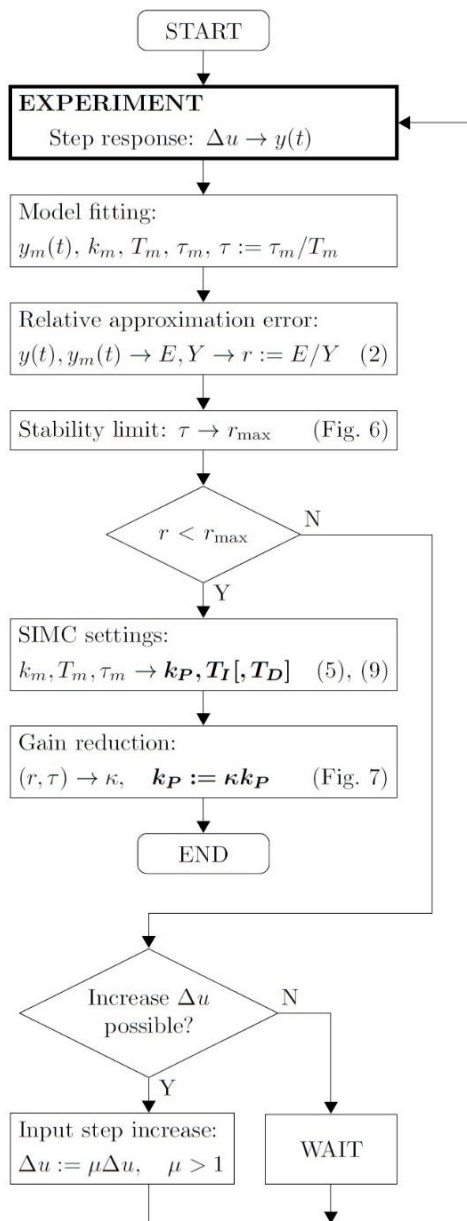

Fig. 8. Algorithm for tuning the controller from a disturbed step response

6. LAB EXPERIMENT

6.1. Equipment set up and operation

A simple lab set up (Fig. 9) has been assembled to demonstrate the proposed approach in two long experiments, one for open loop and the other for closed loop, involving repeatable tests under varying load disturbances. The set up involves a heating resistor kept in open air, Pt100 temperature sensor, transducer, PWM switch and an embedded system board connected to PC running MATLAB. The embedded system filters the measurements, works as the temperature controller, generates a PWM output signal and supervises the whole operation. Ambient temperature drift (daily cycle) is treated as a slowly varying load disturbance, although unexpected jumps caused, e.g. by opening the door or window, also happen for time to time. The basic open-loop experiment consists of 50 uninterrupted up-down step tests (100 responses in total) triggered automatically by the embedded system. The system continuously records the temperature in a file sent to the PC for identification. A second-order Butterworth filter with 10 s time constant is applied for measurement of the noise rejection.

For a nominal PWM = 25%, the resistor temperature is about 76 °C. After increasing the PWM to 27%, the temperature is recorded for 30 min, which is the t_H time in the integrals Eq. (2a). Such a modest 2% increase may correspond to technological restrictions in an industrial case. After waiting for 30 min, the input is decreased back to 25% and the down-response recorded again. Two up-down temperature changes of the plant and the models are shown in Fig. 10 to clarify the tests. The model output stops at the t_H time of Eq. (2a) followed by waiting. The whole experiment takes 100 h. The average up-down temperature change is 2.7 °C.

6.2. Verification of the disturbance model

Verification that the low-pass filter driven by white noise (Fig. 1(b)) can be a suitable model of the load disturbance is one of the objectives of the open-loop experiment. The verification involves three steps:
- Execution of 50 up-down tests with identification of the parameters $\{k_m, T_m, \tau_m\}$ by means of lsqcurvefit.
- Evaluation of the averages $\{\bar{k}, \bar{T}, \bar{\tau}\}$ treated as parameters of the plant for additional simulation.
- Selection of the low-pass filter parameters $\{n, \sigma_l\}$ to get a similar frequency spectrum of the real and simulated plants.

Histograms of the identified parameters are presented in Fig. 11. Parameter averages are the following

$$\bar{k} = 1.37\,°C/PWM_\%, \quad \bar{T} = 230\,s, \quad \bar{\tau} = 67\,s. \qquad (21)$$

To verify the load disturbance model, the multiplier n in the filter time constant $n\bar{T}$ and the standard deviation σ_l of the white noise are determined by adjusting the simulated frequency spectrum to the real one by using FFT [33]. The resulting estimates are

$$n^* = 32, \quad \sigma_l^* = 10\,PWM_\% \qquad (22)$$

(σ_l^* in control units).

The two spectra after adjustment of the disturbance model are shown in Fig. 12(a), where peaks represent odd harmonics of the up-down changes. The spectra practically overlap which confirms that the transfer function $1/(n^*\bar{T}s + 1)$ driven by white noise with the standard deviation σ_l^* models the load disturbance in the experiment quite well. Change of n would increase $(n > n^*)$ or decrease $(n < n^*)$ the slope of the simulated spectrum. Improper value of the standard deviation σ_l moves this spectrum up or down (Fig. 12(b)). The frequency range 0–1 mHz corresponds to harmonic components with periods above 1,000 s covering 4 time constants $\bar{T}$ $(4\bar{T} = 920)$. A rather large value of n^* is obtained here, so half a decade over $n = 10$ used before may be a hint for simulation of other processes subject to load disturbance.

6.3. Controller design and closed loop

The histogram of the distribution of r for the 100 recorded step responses is shown in Fig. 13a. Out of the responses, six have not passed the acceptance test, Eq. (20). Exemplary data from one of the accepted responses consist of the FOPTD parameters $k_m = 1.37\,°C/PWM_\%$, $T_m = 266\,s$, $\tau_m = 66.8\,s$ and the integrals $Y = 81.8\,°C \cdot s$, $E = 1.24\,°C \cdot s$ in Eq. (2a). So, we have the normalised delay $\tau = \tau_m/T_m = 0.296$ and the relative approximation error $r = E/Y = 0.0152$ $(r_{max} = 0.026$ from Fig. 6). The SIMC rules Eq. (11) give the initial PI settings $k_P = 1.23$ and $T_I = 226$. Having r and τ, the value of the gain reduction factor κ read out from Fig. 7a is 0.48 (after some interpolation). Hence, the controller gain is reduced to $\kappa k_P = 0.592$.
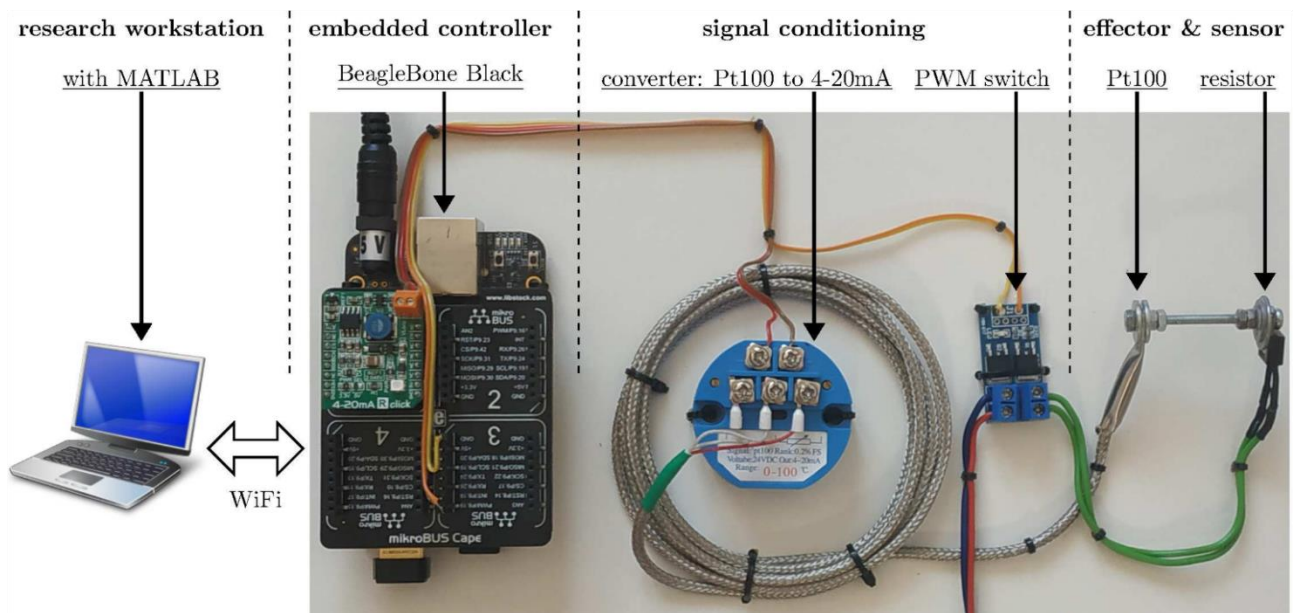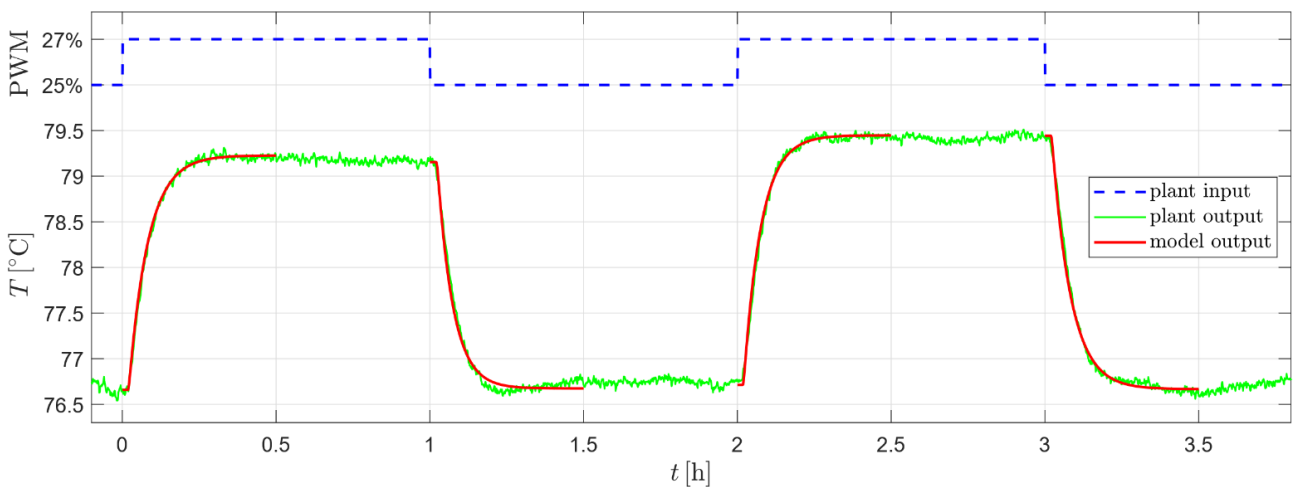

Fig. 9. Equipment set up

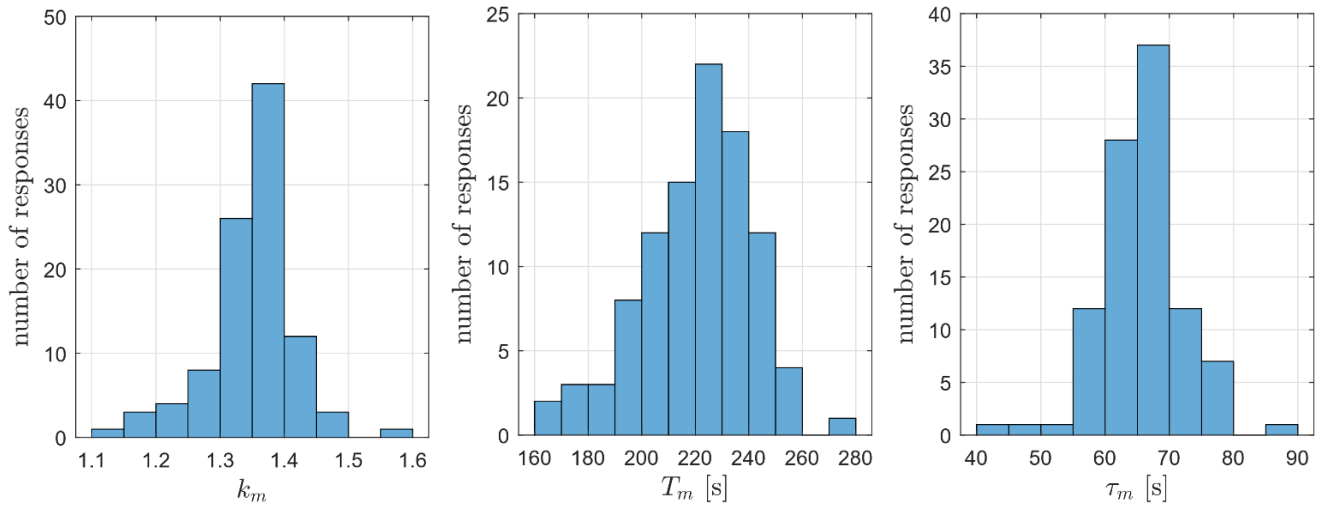**Fig. 10.** Two exemplary up-down step responses

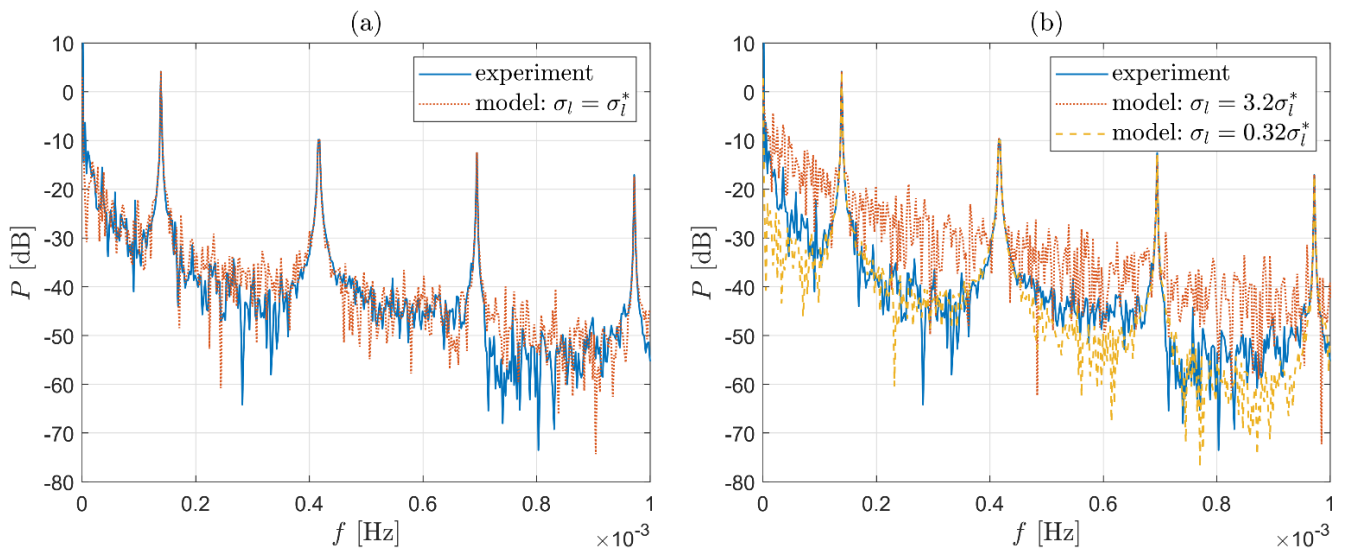**Fig. 11.** Histograms of the identified parameters

Fig. 12. Frequency spectra of the real and simulated plant outputs: (a) after adjustment of the disturbance model, (b) for improper standard deviation σ_l
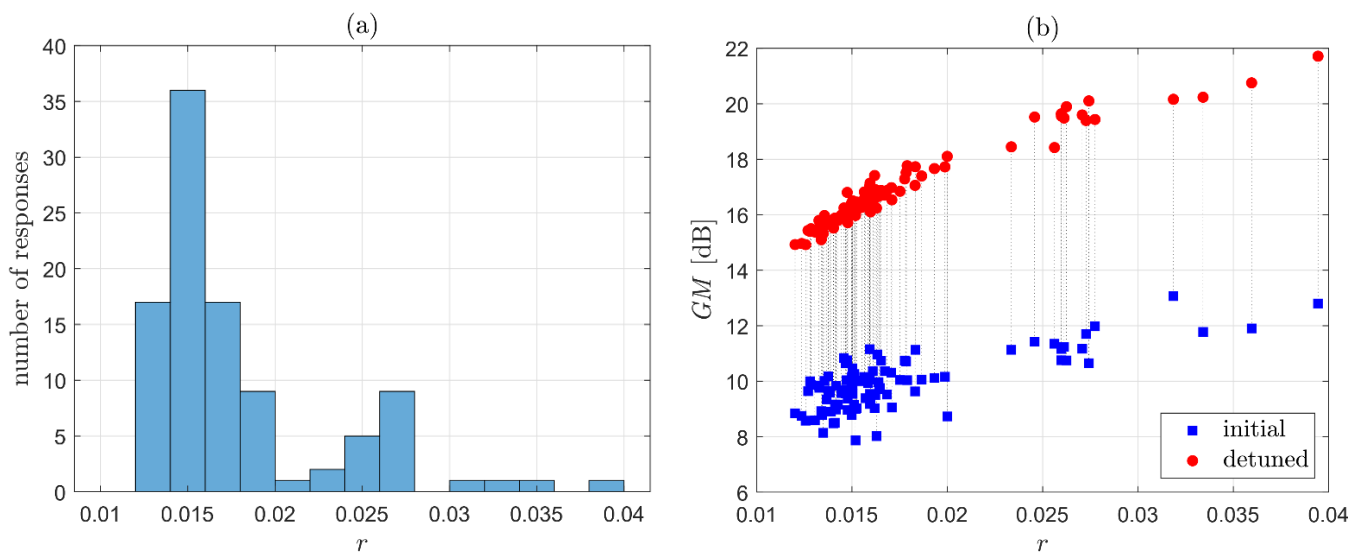

Fig. 13. (a) Number of step responses in terms of the relative error r, (b) gain margins for the initial and detuned settings
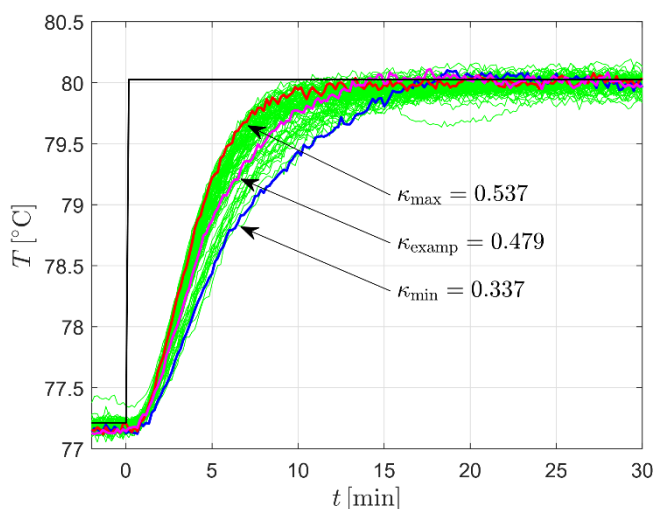
Fig. 14. Detuned closed-loop responses

The resulting closed-loop responses of the real plant recorded in the second experiment are shown in Fig. 14 for the 80 °C setpoint. The case for κ_{examp} relates to the exemplary calculations given above. The responses are smooth and settle down in a fairly similar time. The reduction factor assumes values from $\kappa_{\min} = 0.337$ to $\kappa_{\max} = 0.537$. Note that $\kappa_{\min}$ is close to the stability limit $1/\pi \cong 0.318$.

By taking the average parameters in Eq. (21) as plant data, one can check how the gain margins look like before and after the reduction. Lower squares in Fig. 13(b) represent the initial margins. Some of them are below the nominal 10 dB. The reduction increases the margins by 5–8 dB depending on the relative error r.

The presented results are obtained for rather a small input step $\Delta \mathrm{PWM} = 2\%$ to reflect technological restrictions. A larger step would decrease values of the error r thus, increasing the reduction factor κ. For $\Delta \mathrm{PWM} = 5\%$ the values of r do not exceed 0.012, giving $\kappa_{\min} = 0.568$ and $\kappa_{\max} = 0.863$.

The PID controller for the SOPTD model is not implemented since due to the smaller $r_{\max}$ (Fig. 6), too many step tests do not pass the acceptance condition in Eq. (20). Besides, the reduction factor κ is much smaller.

Finally, we explain why the identified $n^* = 32$ for the low-pass filter has not been used, although possible in this particular case. In a practical situation, an engineer only knows that the load disturbance interferes at lower frequencies in relation to process dynamics, but does not know exactly how much. Therefore, the approach with $n = 10$, justified by the similar plots in Fig. 4, seems an appropriate solution.

7. CONCLUSIONS

Due to technological restrictions, the step response required for controller tuning is sometimes triggered when the process is not in a steady-state or is subject to major load disturbance. This means that the parameter estimates obtained from the response and corresponding controller settings are not quite reliable. Hence, to avoid possible poor behaviour of the closed-loop system, the settings must be detuned, typically by reducing the gain. It is up to the engineer's experience to decide by how much to reduce.

FOPTD and SOPTD processes have been considered with the load disturbance modeled by a low-pass filter driven by white noise. Process parameters are determined by the least-squares curve fitting, so the estimation error of the response indicates to what extent the process is not in a steady-state or disturbed. Relative approximation error relates the error to the step response and is a basic data for reducing the gain.

SIMC rules have been applied to tune PI and PID controllers for FOPTD and SOPTD, respectively, taking process delay as the recommended closed-loop time constant. By repeating the tests in a long, uninterrupted simulation, the case with the lowest gain margin is detected and used subsequently for detuning. Final nomograms specify by how much to reduce the initial controller gain given a relative approximation error and process delay. So contribution of this paper rests in the precise evaluation of the gain reduction to assist the engineer.

Low-frequency load disturbance model has been verified in a simple, yet long, lab experiment with multiple step tests.

The MATLAB lsqcurvefit function has been used for identification. Ultimately however, the approach is supposed to be transferred from the embedded system board into a PLC-based process control equipment [34]. In such a case, a corresponding code may be written in structure text language of IEC 61131-3 standard [35] applying the two-stage curve-fitting algorithm from [15,16] for identification.

Research on the controller retuning directly in a closed-loop system subject to load disturbance is left for future work.

REFERENCES

1. Åström KJ, Murray RM. Feedback Systems: An Introduction for Scientists and Engineers. Princeton: Princeton University Press; 2008.
2. Seborg DE, Edgar TF, Mellichamp DA, Doyle FJ. Process Dynamics and Control, 4th Edition. New York: Wiley; 2016.
3. Åström KJ, Hägglund T. Advanced PID Control. Research. Triangle Park; 2005.
4. Liu T, Wang QG, Huang HP. A tutorial review on process identification from step or relay feedback test. Journal of Process Control. 2013; 23(10):1597-1623.
5. Skogestad S. Simple analytic rules for model reduction and PID controller tuning. Journal of Process Control. 2003; 13(4):291-309.
6. Ljung L. System Identification: Theory for the User, 2nd Edition. New York: Prentice Hall; 1999.
7. Söderström T, Stoica P. System Identification, 2nd Edition. New York: Prentice Hall; 2001.
8. Ahmed S., Huang B, Shah SL. Novel identification method from step response. Control Engineering Practice. 2007; 15(5):545-556.
9. Ahmed S, Huang B, Shah SL. Identification from step responses with transient initial conditions. Journal of Process Control. 2008; 18(2):121-130.
10. Liu T, Huang B, Qin SJ. Bias-eliminated subspace model identification under time-varying deterministic type load disturbance. Journal of Process Control. 2015; 25:41-49.
11. Hou J, Liu T, Wang QG. Recursive subspace identification subject to relatively slow time-varying load disturbance. International Journal of Control. 2017; 91(3):622-638.
12. Dong S., Liu T, Wang W, Bao J, Cao Y. Identification of discrete-time output error model for industrial processes with time delay subject to load disturbance. Journal of Process Control. 2017; 50:40-55.
13. Li LJ, Dong TT, Zhang S, Zhang XX, Yang SP. Time-delay identification in dynamic processes with disturbance via correlation analysis. Control Engineering Practice. 2017; 62:92-101.

14. Kon J, Yamashita Y, Tanaka T, Tashiro A, Daiguji M. Practical application of model identification based on ARX models with transfer functions. Control Engineering Practice. 2013; 21(2):195-203.

15. Hwang SH, Lai ST. Use of two-stage least-squares algorithms for identification of continuous systems with time delay based on pulse responses. Automatica. 2004; 40 (9):1561-1568.

16. Yan R, Liu T, Chen F, Dong S. Gradient-based step response identification of overdamped processes with time delay. Systems Science & Control Engineering. 2015; 3(1):504-513.

17. RamVD, Chidambaram M. On-line controller tuning for critically damped SOPTD systems. Chemical Engineering Communications. 2014; 202(1):48-58.

18. Du YY, Tsai JS, Patil H, Shieh LS, Chen Y. Indirect identification of continuous-time delay systems from step responses. Applied Mathematical Modelling. 2011; 35(2):594-611.

19. Liu Q, Shang C, Huang D. Efficient low-order system identification from low-quality step response data with rank-constrained optimization. Control Engineering Practice. 2021; 107:104671.

20. Jin Q, Liu Q, Huang B. Control Design for Disturbance Rejection in the Presence of Uncertain Delays. IEEE Transactions on Automation Science and Engineering. 2017; 14(4):1570-1581.

21. Sung SW, Lee J, Lee IB. Process Identification and PID Control. Wiley-IEEE Pres. 2009.

22. Sun L, Xue W, Li D, Zhu H, Su Z. Quantitative tuning of active disturbance rejection controller for FOPTD model with application to power plant control. IEEE Transactions on Industrial Electronics. 2022; 69(1):805-815.

23. O'Dwyer A. Handbook of PI and PID Controller Tuning Rules, 3rd Edition. Imperial College Press; 2009.

24. Dahlin EB. Designing and tuning digital controllers. Instruments and Control Systems. 1968; 41(6):77-83.

25. Rivera DE, Morari M, Skogestad S. Internal model control: PID controller design. Industrial & Engineering Chemistry Process Design and Development. 1986; 25(1):252-265.

26. Veronesi M, Visioli A. Performance Assessment and Retuning of PID Controllers. Industrial & Engineering Chemistry Research. 2009; 48(5):2616-2623.

27. Grimholt C, Skogestad S. Optimal PI and PID control of first-order plus delay processes and evaluation of the original and improved SIMC rules. Journal of Process Control. 2018; 70:36–46.

28. Veronesi M, Visioli A. Improving lambda tuning of PI controllers for load disturbance rejection. In Proceedings of the 26th IEEE International Conference on Emerging Technologies and Factory Automation (ETFA); 2021; 1-6.

29. Hägglund T. A unified discussion on signal filtering in PID control. Control Engineering Practice. 2013; 21(8):994-1006.

30. Oliveira PM, Hedengren JD. An APMonitor temperature lab PID control experiment for undergraduate students. In Proceedings of the 24th IEEE International Conference on Emerging Technologies and Factory Automation (ETFA). 2019; 790-797.

31. Veronesi M, Visioli A. On the Selection of Lambda in Lambda Tuning for PI(D) Controllers. IFAC-PapersOnLine. 2020; 53(2):4599-4604.

32. Saxena S, Hote YV. Stabilization of perturbed system via IMC: An application to load frequency control. Control Engineering Practice. 2017; 64:61-73.

33. Pintelon R, Schoukens J. System Identification: A Frequency Domain Approach, 2nd Edition. Wiley; 2012.

34. Rzońca D, Sadolewski J, Stec A, Świder Z, Trybus B, Trybus L. Developing a multiplatform control environment. Journal of Automation, Mobile Robotics and Intelligent Systems. 2019; 13(4):73-84.

35. EN 61131-3, Programmable controllers – Part 3: Programming languages (IEC 61131-3:2013), International Standard; 2013.

Andrzej Bożek: https://orcid.org/0000-0003-3015-7474

Leszek Trybus: https://orcid.org/0000-0002-1415-3679